Deltoid vs. Rhomboid: Controlling the Shape of bis-Ferrocene Macrocycles by the Bulkiness of the Substituents

Journal:	*Organometallics*
Manuscript ID	om-2016-00909f.R1
Manuscript Type:	Article
Date Submitted by the Author:	06-Jan-2017
Complete List of Authors:	Hoffmann, Viktor; University of Basel, Department of Chemistry Le Pleux, Loïc; University of Basel, Department of Chemistry Häussinger, Daniel; Universität Basel, Chemie Unke, Oliver; University of Basel, Department of Chemistry Prescimone, Alessandro; University of Basel, Chemistry Mayor, Marcel; University of Basel, Department of Chemistry

Deltoid vs. Rhomboid: Controlling the Shape of *bis*-Ferrocene Macrocycles by the Bulkiness of the Substituents

Viktor Hoffmann,† Loïc le Pleux,† Daniel Häussinger,† Oliver T. Unke,† Alessandro Prescimone,† and Marcel Mayor,*†‡§

†University of Basel, Department of Chemistry, St. Johanns-Ring 19, CH-4056 Basel, Switzerland

‡Karlsruhe Institute of Technology (KIT), Institute of Nanotechnology (INT), P.O.Box 3640, D-76021 Karlsruhe, Germany.

§Lehn Institute of Functional Materials (LIFM), Sun Yat-Sen University, Guangzhou, China.

ABSTRACT: Precise structural control of heteroannularly disubstituted ferrocene (Fc) structures is very challenging as the high rotational mobility of the Fc unit allows a large conformational diversity. Herein we present the syntheses, characterization and electrochemical investigation of two complementary *bis*-ferrocene macrocycles, built up via Sonogashira cross coupling and intramolecular ring closing reaction. While the X-ray structure of 1,2-ethynylbenzene bridged *bis*-ferrocene complex **1** shows a *deltoidal* conformation, a stretched oriented *rhomboidal bis*-ferrocene metallacycle **2** is formed, when the peripheral benzene rings are decorated with bulky *tert*-butylsulfanyl groups. VT-NMR spectroscopy is used to assign the rotation of the embedded Fc units in *rhomboid* **2**. Moreover, cyclic voltammetry (CV) of *deltoid* **1** and *rhomboid* **2** indicate that electronic communication between both ferrocenyl groups can be neglected, while the electrostatic through space coupling is significant.

Introduction.

Over the past few decades, fascinating macrocycles comprising ferrocenes as functional units have been reported such as a molecular scissors,[1] tweezers[2] and springs.[3] Chiral structures resembling Escher`s endless staircase[4] or ferrocene (Fc) terminated helicene[5] are remarkable examples of how the 3-dimensional scaffold of ferrocene is used as structure providing "shaping" synthon. Moreover, the stable and reversible redox chemistry of ferrocene has been exploited in molecular wires,[6] sensors,[7] and switches.[8] Furthermore, substituents on the cyclopentadienyl (Cp) rings enable the fine-tuning of the energy states involved. Owing to its extensive use in numerous areas of applied science, we became interested in the structural control over the embodied ferrocene units as part of the functional application.[9] We experienced the precise construction of discrete and shape-persistent ferrocene macrocycles as challenging, in particular when ferrocene is integrated as heteroannularly disubstituted subunit and the Cp-Fe-Cp junction is part of the macrocycle such that its rotational freedom allows for a large structural diversity.

Along these considerations, we became interested in macrocycles comprising two ferrocene units which on the one side will increase the structural variation problematic, but on the other hand give access to potentially mixed-valence compounds with exciting intramolecular redox properties. To minimize the structural diversity and to maximize the extent of Coulomb interactions between both ferrocene subunits, *bis*-Fc macrocycles consisting of small and rigid scaffolds moved into the focus of interest. Due to our experience with macrocycles consisting of ethynyl interlinked aryl subunits,[10–15] we became interested in 1,2-diethynylbenzene bridges to combine two Fc subunits in a compact fashion favoring intramolecular Coulomb interactions. Such a linker was already reported by Diallo et al., where in a series of Fc terminated compounds, 1,2-*bis*(ferrocenylethynyl)-benzene (**3** in Figure 1) exhibited interesting electrostatic interaction characteristics.[16] In their study they showed that the two ferrocenyl groups turn out of plane in order to minimize the electrostatic repulsion upon oxidation. This pioneering study even increased our interest in cyclic derivatives, as the fixation of the Fc subunits within a macrocyclic framework should limit their ability to sidestep in order to avoid electrostatic repulsion. Interestingly, two macrocyclic structures comprising two ferrocenes heteroannularly interlinked by two *ortho*-diethynyl benzene linkers are possible, which are both presented in this work.

In particular, we describe the syntheses, full characterization, and electrochemical investigation of the *deltoidal* shaped *bis*-ferrocene **1** with both *ortho*-diethynyl benzene linkers stacked, on top of each other which we thus enti-

tled *"deltoid"*, and of the macrocycle **2**, with both *ortho*-diethynyl benzene linkers on opposed sides of the double Fc junction, which we simply call *"rhomboid"* in the following of the paper. In the case of the *rhomboid* **2** we further analyze the dynamic structural behavior by NMR-analyses. Both target structures differ in their spatial arrangement and consequently also in the symmetry elements involved. As the R-substituents of the *deltoid* **1** are hydrogen atoms, the structure has a mirror plane comprising both Fe-atoms of the ferrocene junctions and a C_2-axis going through the middle of the connection between both Fe-atoms and a point in the middle between both parallel benzene units. In the case of the *rhomboid* **2**, both R-substituents are bulky *tert*-butylsulfanyl groups and the symmetry element is an inversion point between both Fe-atoms of the ferrocene junctions.

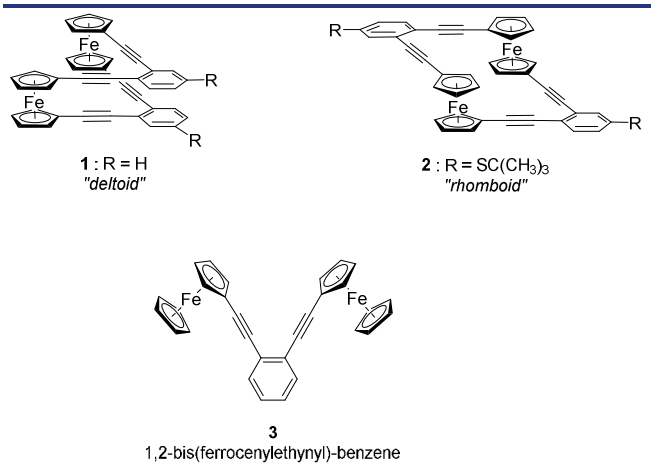

Figure 1. Structures of the *bis*-ferrocene macrocycles "*deltoid*" **1** and "*rhomboid*" **2**, together with 1,2-*bis*(ferrocenyl-ethynyl)-benzene **3**.

Cyclization Strategy.

After several unsuccessful attempts to assemble *bis*-ferrocene macrocycles by dimerizing suitably functionalized ferrocene derivatives, we decided for a step-wise assembly of both bridging linkers. While such a synthetic strategy guarantees for good control over the formed connections, it comes with a considerable increase in the number of consecutive reaction steps required, even comprising statistical steps with limited atom economy. On the other hand, the subsequent formation of the second linker can also be considered as opportunity to control the spatial arrangement of the macrocycle. As sketched in Scheme 1, the Fc-junctions and the ethynyl linkers can be considered as rotating joints giving access to both structures, the *deltoid* and the *rhomboid*. In the precursor of the *deltoid* (Scheme 1, right side on the top), the two benzene rings are arranged parallel on top of each other stabilized by stacking interactions, as already reported e.g. in the solid state structures of 1,1'-*bis*(phenylethynyl)ferrocene[17] and further decorated derivatives thereof.[9,18] On the other hand, potential substituents (R in Scheme 1) come in close proximity in the *deltoid* precursor and the steric repulsion probably disfavors this conformer when large enough substituents are involved. Instead the rotational motions around the ferrocene and ethynyl joints might favor a conformer enabling the ring-closing reaction on the opposed side, resulting in the desired *rhomboid*. The equilibrium between both precursors should depend on the balance between attractive stacking interactions and steric repulsion, which should be adjustable by the choice of the substituent R.

The assembly of the macrocycles and their precursors is based on a combination of acetylene scaffolding strategies[19] and the well-developed Sonogashira-type coupling chemistry with ferrocene building blocks.[16,18,20–22] As the substituent R is selected on an early stage of the stepwise assembly strategy, each macrocycle has to be synthesized from scratch.

Scheme 1. Equilibrium between two conformers during the ring-closing reaction, which are expected to yield each in another well-defined structure, namely either the *deltoid* or the *rhomboid*. The bulkiness of the substituent R might serve as trigger to favor one conformer over the other and consequently also direct the resulting macrocycle.

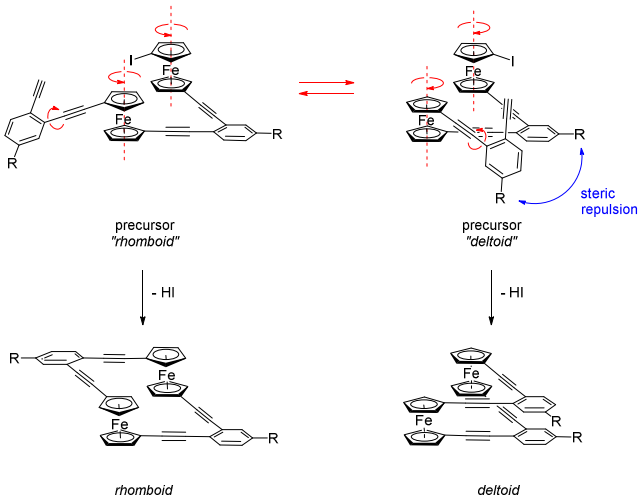

To scrutinize the hypothesis presented in Scheme 1, we focused on two model compounds each favoring one of the two precursor conformers. In order to favor the *deltoid* conformation, the steric interaction between both R-groups has to be minimized and we thus decided to get rid of the substituent (R = H in **1**). To steer the precursor equilibrium towards the *rhomboid* conformation, the bulky *tert*-butylsulfanyl group has been selected (R = S^{t}Bu in **2**). The bulkiness of the substituent was not the only selection criteria, the *tert*-butylsulfanyl substituent can also be considered as a masked thiol anchor group which might become interesting to integrate the macrocycle in future single molecule junction experiments.

Results and discussion.

Synthesis.

As already mentioned above, the macrocycles were synthesized in a step-wise assembling strategy consisting of repetitive reaction sequences consecutively closing one linker after the other. As key building block the properly masked 1,2-diethynylbenzene derivative was required. To optimize both, chemical control and synthetic flexibility, an orthogonal pair of ethynyl protection groups was desired. The combination triisopropylsilyl (TIPS) and 2-hydroxypropyl (HOP) as ethynyl masking groups reported by Kukula et al.[23] was ideally suited for the purpose. The synthesis of the *deltoid* **1** is displayed in Scheme 2. The monoprotected 1,2-diethynylbenzene derivative **5** was prepared by successive Pd-catalyzed coupling of 1-bromo-2-iodobenzene with 2-methyl-3-butyn-2-ol and (triisopropylsilyl)acetylene profiting from the difference in reactivity of the two halogen substituents, followed by removal of the triisopropylsilyl protection group by treatment with a 1 M TBAF solution. We recently reported[9] the high-yield experience we made in C-C coupling reactions between 1,1'-diiodoferrocene (**6**) and acetylenes with the palladium/phosphine couple[24] elaborated by Inkpen et al.[21] For the assembly of Fc-macrocycles reported here, we used the corresponding air-stable trialkylphosphonium salt,[25] since preliminary studies showed that the advantages in handling and storage outbalanced the moderate loss in yields. We thus treated 1,1'-diiodoferrocene **6** with 3 equivalents of the acetylene **5** in the presence of catalytic amounts of $Pd(MeCN)_2Cl_2$, $[(t\text{-}Bu)_3PH]BF_4$, and CuI in a THF/DIPA mixture at 60 °C for 12 h. After aqueous work-up the reaction products were isolated by flash column chromatography (FCC) on silica gel. As main product, the 1,1'-diethynyl-substituted ferrocene derivative **8** was isolated in 47% yield, together with 23% of the singly ethynyl-substituted compound **7**. We were particularly interested in the doubly HOP protected diacetylene **8**, as considerable differences in the R_f values of the compounds as a function of the number of polar protection groups were expected. This enables the chromatographic separation of the differently protected compounds, an important feature when statistical deprotection reactions are considered. And indeed, treatment of the doubly HOP protected diacetylene **8** with a *n*-Bu_4NOH solution in degassed toluene for 1 h at 70 °C provided the monoprotected derivative **9** in very good 60% isolated yield after FCC. In order to favor the decoration of the free ethynyl group of **9** with an additional 1-iodo-1'-yl ferrocene unit, a fivefold excess of the 1,1'-diiodoferrocene was used for the coupling between **9** and **6**. Apart from the ratio of the coupled reagents, similar reaction conditions as described above for the coupling between **5** and **6** were applied. After work-up, the desired open chain *bis*-ferrocene derivative **10** was isolated in 39% yield by FCC. The major side product we observed was the oxidative acetylene coupling product providing the diethynyl interlinked Fc-dimer **12** in 12% yield. Despite extensive precautions to exclude oxygen and air from the reaction

Scheme 2. Linear 7 step synthesis of the *deltoid bis*-ferrocene metallacycle 1.[a]

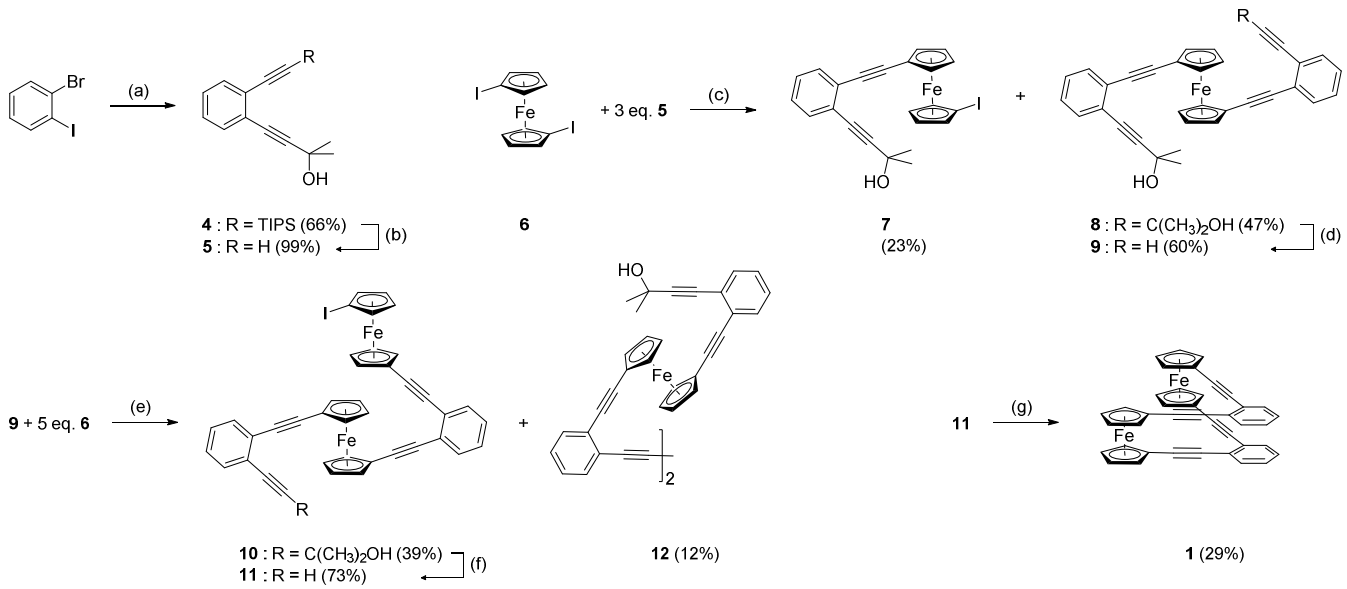

[a]Reagents and conditions: (a) (i) $Pd(PPh_3)_2Cl_2$, CuI, NEt_3, 2-methyl-3-butyne-2-ol, 50 °C, 3 h, (ii) TIPSA, 90 °C, 12 h; (b) TBAF, THF, 25 °C; (c) $Pd(MeCN)_2Cl_2$, $[(t\text{-}Bu)_3PH]BF_4$, CuI, THF/DIPA, 60 °C, (d) TBAOH, toluene, 70 °C 1 h; (e) FcI_2, $Pd(MeCN)_2Cl_2$, $[(t\text{-}Bu)_3PH]BF_4$, CuI, THF/DIPA, 60 °C, (f) TBAOH, toluene, 70 °C; (g) $Pd(MeCN)_2Cl_2$, $[(t\text{-}Bu)_3PH]BF_4$, CuI, THF/DIPA, 1.5 mM in [**11**], 60 °C.

mixture, the formation of **12** could not be suppressed and might originate from the activation cycle forming the catalytically active Pd(0) species. The remaining HOP protection group in **10** was removed again by treatment with a *n*-Bu_4NOH solution in degassed toluene at 70 °C for 3 h, and the free acetylene **11** was isolated as orange solid in 73% yield after FCC. With the terminal acetylene and iodoferrocene functionalized *bis*-ferrocene derivative **11**, the ideal precursor for the intramolecular Sonogashira reaction as cyclization step was available. To perform the cyclization step, a 1.5 mM solution of **11** in a THF/DIPA mixture was prepared and treated with the same reagents and conditions described above for the coupling between **5** and **6**. After work up, we isolated as only reaction product formed in reasonable yields the *deltoid bis*-ferrocene metallacycle **1** as pale orange solid in 29% yield. The remaining material probably forms larger oligo- and polymers which were not isolated. The target structure **1** displayed very limited solubility features in all organic solvents investigated and we were initially afraid of facing challenging boundary conditions for its characterization. But we were pleased to realize that its poor solubility is reflected in its pronounced tendency to crystallize and single crystals suitable for X-ray analysis were obtained by slow evaporation of a solution of **1** in dichloromethane.X-ray crystallography unambiguously corroborated the identity of the compound **1** and displayed its conformation (Figure 2). The *bis*-ferrocene **1** has C_2 symmetry and resembles the expected *deltoidal* shaped geometry, with small deviations from the geometrical ideal arrangement of an isosceles triangle, with enclosed angles of 61.01° and 66.13°, respectively. The deviation is caused by one ferrocene unit, which is inclined with respect to the aryl plane by ~ 7°, while the other ferrocene is almost in plane. The iron centers are almost coplanar, based on Cp centroid-Fe1-Fe2 enclosed angle of 89.32°, and separated by only 7.116 Å. The interplanar phenyl distance is with 3.577 Å slightly longer than the Cp-Cp distance (3.311 Å) and both phenyl rings are sitting on top of each other. In addition, the two Fe atoms and the center between the phenyl rings share a plane of symmetry due to their parallel arrangement and fixation in the *bis*-metallacyclic framework. *Deltoid* **1** was further characterized by ^1H and HMBC NMR spectra and MALDI-ToF mass spectrometry. Due to the poor solubility of **1** we were not able to record meaningful ^{13}C NMR spectra.

The exclusive formation of the *syn*- conformation supports the first part of our working hypothesis, namely that in the absence of steric restriction the *deltoid bis*-metallacycle is favored. Bulky substituents (*tert*-butyl and *tert*-pentyl) are known to restrict the revolving motion of the Cp rings in ferrocene model compounds.[26] The comparable spacing between both phenyl rings and the Cp rings in the solid state structure of **1** suggested that substituents of comparable dimensions should be bulky enough to handicap the *syn*- arrangement and steer the ring-closing reaction towards the *rhomboidal anti*- conformation. As already motivated in the "cyclization strategy" section above, we chose *tert*-butylsulfanyl groups as R substituents combining the required bulkiness with promising features as potential anchor groups. It is noteworthy that our initial approach considering even bulkier triphenylmethylsufanyl groups failed, due to severe deactivation of the triphenylmethylsufanyl decorated aryl system in the subsequent C-C coupling reactions.

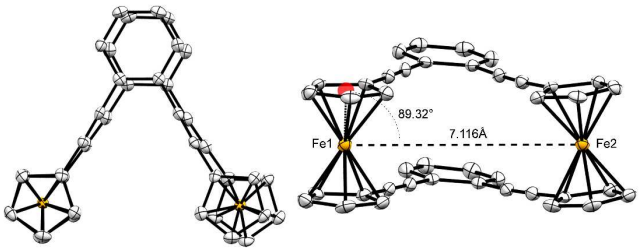

Figure 2. Solid state structure of the *deltoid* **1**. ORTEP plots with ellipsoids plotted at the 50% probability level (hydrogen atoms are omitted for clarity).

The synthesis of the *rhomboid* **2** is displayed in Scheme 3. The assembly of the *ortho*-diethynylbenzene building block started with the regioselective oxidative thiocyanation of 2-iodoaniline in *para*-position, using Oxone® and ammonium thiocyanate, which provided 2-iodo-4-thiocyanato-aniline **13** in excellent yield.[27] Aniline **13** was readily sublimed in batch scales of up to 15 g and was converted to the bromo derivate **14**, using Cu(II) bromide and *tert*-butyl nitrite[28] in a 5:1 ratio of acetonitrile/methylene chloride. Reduction of thiocyanate using LAH to provide the free thiol which was alkylated with 2-chloro-2-methylpropane in the presence of catalytic amounts of aluminum chloride to yield **15** in 76% over both steps. With the bromo-iodo-aryl derivative **15** in hands, the different reactivity of both halides in Pd-catalyzed Sonogashira coupling allows for the subsequent coupling with two differently protected acetylene derivatives in a single reaction step. Thus **15** together with both catalysts $(Pd(PPh_3)_2Cl_2$ and CuI were dissolved in a degassed 3:1 THF/NEt_3 mixture and 2-methyl-3-butyn-2-ol was added at 25 °C. After 3 h the monitoring of the reaction mixture by thin layer chromatography (TLC) displayed the complete consumption of the acetylene and (triisopropylsilyl)acetylene was added and the reaction mixture was heated at 80 °C over night (16 h). FCC of the concentrated crude reaction mixture provided the differently protected diethynyl **16** in 81% yield. The orthogonal protection groups enable either the removal of triisopropylsilane or the hydroxypropyl and thus the perfect control over the demasking of the ethynyl groups in *para*- and *meta*-position respectively. The doubly protected diethynyl **16** was either treated with fluoride ions in wet THF to give the singly HOP protected diethynyl **17** in good yield, or it was exposed to *n*-Bu_4NOH in degassed toluene at 70 °C for 3 h to provide the singly TIPS protected diethynyl **18** in good yields. Either one of the iodine atoms of 1,1'-diiodoferrocene had to be substituted consecutively by one of the two mono-protected diethynyls **17** and **18**. This is particular important to control the symmetry of the tar-

geted *rhomboid bis*-ferrocene metallacycle, as the substitution of both iodines of **6** with the same mono-protected diethynyl would yield after ring closure in a *rhomboid* metallacycle with C_2 symmetry instead of the here desired C_i symmetry. To favor mono-substitution, the HOP-masked diethynyl **17** was treated with a 3-fold excess of 1,1'-diiodoferrocene using the already described Sonogashira coupling conditions, providing the mono-substituted iodoferrocene **19** in moderate isolated yields of 37%.

In contrast to our prior experience with this catalytic system, the reaction progress was slower and we observed notable quantities of dehalogenated ferrocene derivatives. We thus altered the catalytic system to $Pd(dppf)Cl_2$ with copper(I) iodide for the next coupling and added the TIPS-masked diethynyl **18** in a slight excess to the preheated mixture of **19** dissolved in DIPA/THF. After keeping the reaction mixture at 70 °C for 4 h, the desired doubly substituted Fc derivative **20** was isolated also in moderate yields of 35% by FCC. The ferrocene **20** is again an orthogonally HOP and TIPS protected diethynyl and the TIPS group was efficiently removed by treatment with TBAF in wet THF at 25 °C giving the mono-deprotected diethynylferrocene moiety **21** almost quantitatively. To favor the formation of the open-chain *bis*-ferrocene **22**, the Sonogashira reaction was performed with a 5-fold excess of the diiodoferrocene **6**. The excess of **6** and the catalysts $(Pd(dppf)Cl_2$ and CuI were dissolved in a degassed THF/DIPA (2:1) mixture to which the acetylene **21** dissolved in degassed THF was added. After keeping the reaction mixture for 2 h at 50 °C, the reaction products were isolated by FCC. Besides the desired open-chain *bis*-ferrocene **22**, which was isolated in 38% yield, again the oxidative acetylene coupling product **23** was obtained in 23% despite of all attempts to avoid the presence of oxygen. For the final deprotection, the HOP-ethynyl derivative **22** was treated with *n*-Bu_4NOH in degassed toluene at 70 °C for 3 h to provide the open-chain precursor **24** with an acetylene at one end and an iodoferrocene subunit at the other end.

Scheme 3. Synthesis of the *rhomboidal bis*-ferrocene metallacycle 2 consisting of 11 consecutive steps.[a]

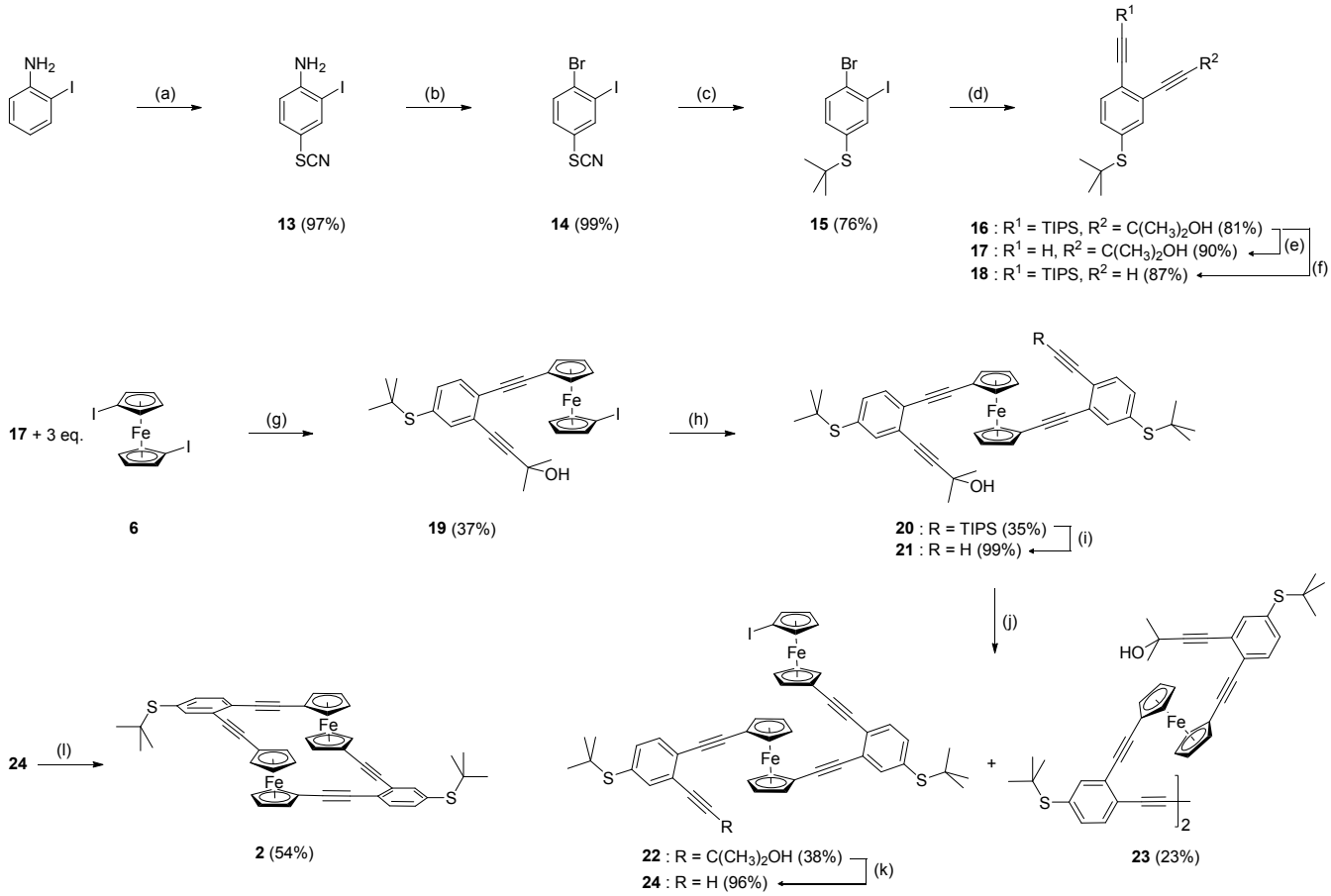

[a]Reagents and conditions: (a) NH_4SCN, Oxone, MeOH, 25 °C; (b) $CuBr_2$, *t*BuONO, MeCN/DCM, 65 °C; (c) (i) LAH, THF, 25 °C (ii) 2-chloro-2-methylpropane, $AlCl_3$, 25 °C; (d) (i) $Pd(PPh_3)_2Cl_2$, CuI, 2-methyl-3-butyn-2-ol, THF/NEt_3, 25 °C., 5 h, (ii) TIPSA, 80 °C, 16 h; (e) TBAF, THF, 25 °C; (f) TBAOH, toluene, 70 °C, 3 h; (g) $Pd(MeCN)_2Cl_2$, $[(t\text{-}Bu)_3PH]BF_4$, CuI, THF/DIPA, 60 °C, (h) $Pd(dppf)Cl_2$, CuI, **18**, THF/DIPA, 70 °C; (i) TBAF, THF, 25 °C; (j) 5 eq. **6**, $Pd(dppf)Cl_2$, CuI, THF/DIPA, 50 °C, 2 h; (k) TBAOH, toluene, 70 °C; (l) $Pd(PPh_3)_4$, DIPA, toluene 0.1 mM in [**24**], 90 °C.

With the open-chain precursor **24** in hands we were striving for exploring suitable cyclization conditions. To our surprise all attempts using typical Sonogashira reaction conditions like e.g. also all the variations used during the assembly of the linkers failed. Independent of the initial concentration of **24** the desired intramolecular cyclization product was not detected, but instead exclusively intermolecular reaction products were found by mass-spectrometric analysis of the reaction mixtures, pointing at oxidative acetylene coupling as main competing reaction. After numerous unsuccessful attempts, we investigated copper-free reaction conditions and were delighted to observe the mass signal pointing at the formation of the macrocycle by an intramolecular C-C coupling reaction. By far the best result was achieved with $Pd(PPh_3)_4$ and DIPA in toluene without an additional copper salt.

A 0.1 mM solution of **24** in degassed toluene together with the Pd catalyst and DIPA was kept at 70 °C for 4 h. FCC of the concentrated crude reaction mixture provided the desired *rhomboid bis*-ferrocenemetallacycle **2** as orange solid in 54% isolated yield.The *rhomboid* **2** was fully characterized by high resolution mass spectrometry, ^{1}H and ^{13}C NMR spectra supplemented by advanced NMR experiments (NOESY, HMBC, HMQC, and VT NMR experiments) to determine the spatial arrangement of the subunits.

Spectroscopic evidence of the *rhomboid* macrocycle.

The two peripheral *tert*-butylsulfanyl groups of the *bis*-ferrocene **2** considerably increased its solubility in polar aprotic solvents (e.g. acetone, DCM, THF, EtOAc, DMF) but also reduced its tendency to crystallize and so far, all attempts to grow single crystals suitable for X-ray analysis failed. It thus remained a spectroscopic challenge to proof its identity, in particular the *rhomboid* macrocyclic structure of the *bis*-ferrocene **2**. Molecular model analyses displayed an interesting feature of the *rhomboidal* arrangement which might be observed by variable temperature NMR (VT NMR) experiments. While the *rhomboid* macrocyclic arrangement of **2** is shape-persistent and cannot interconvert to the *deltoid* arrangement observed for **1**, an additional motion of the macrocyclic framework was expected for **2**.

The freely suspended ferrocene subunits between both phenyl rings mounted with revolving ethynyl joints should enable a rotary motion of each Fc subunit within the macrocyclic framework as sketched in Figure 3a. Thereby, the rotation of a single ferrocene unit by 180° should result in a helical arrangement of the macrocycle with a pseudo C_2 symmetry. It is noteworthy that the term "pseudo" for the symmetry description is only correct if exclusively the macrocyclic structure is

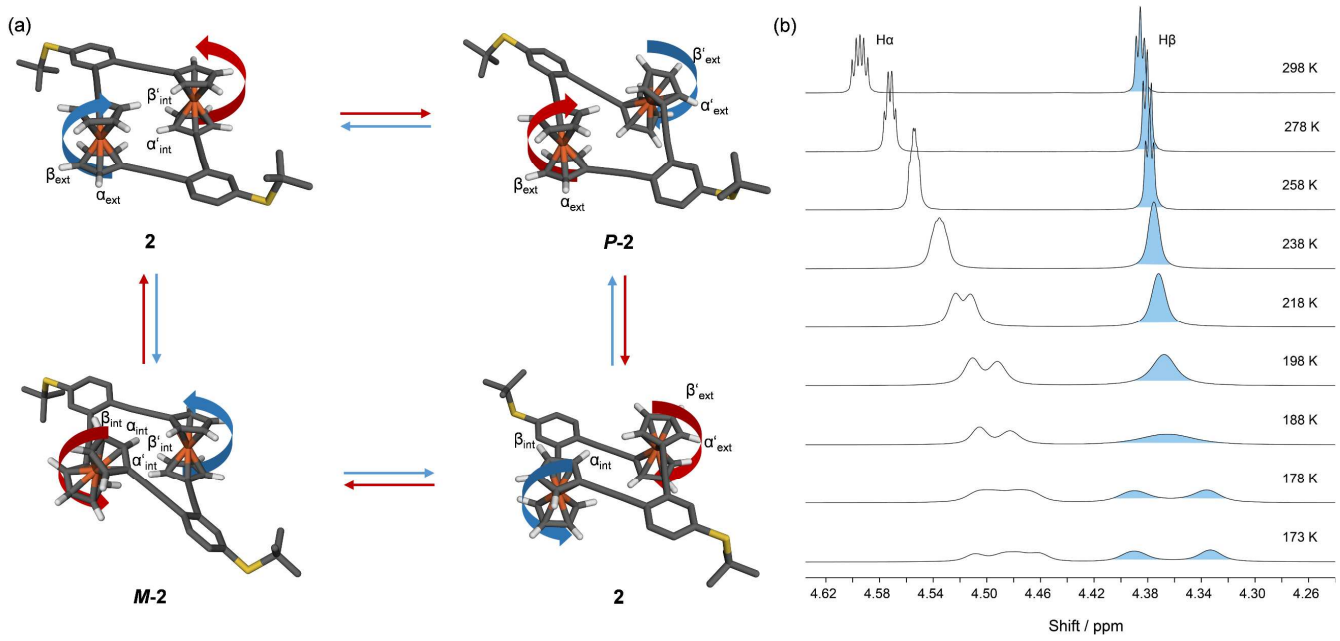

Figure 3. a) Equilibrium between the different conformers of the *rhomboid* **2** accessible via rotational motion of a ferrocene subunit within the macrocycle's framework. Exclusively the *α* and *β* ferrocenyl protons are labelled for visibility. The helical chirality descriptors *P* and *M* refer exclusively to the arrangement of the macrocycle and ignore the peripheral ^{t}BuS-substituent. b) Region of the ferrocene signals of the recorded ^{1}H NMR spectra of **2** in CD_2Cl_2 in a temperature range from 298 K to 173 K. The signals of the *β* ferrocene protons were used for LSA and are highlighted in light blue.

considered and the two peripheral *tert*-butylsulfanyl substituents are ignored. Subsequent rotation of the second ferrocene unit renders the initial conformer. Such a rotation is only possible in the *rhomboid anti*- arrangement and should allow its differentiation from the more rigid stacked *deltoid* arrangement, which does not allow for such motions. Also, the frequency of the rotation is expected to depend on the sample's temperature and might alter the differentiation of the NMR signals of the involved Fc subunits. We thus recorded the ^{1}H NMR spectra of **2** at 25 °C and successively cooled the sample to -100 °C (Figure 3b). At 25 °C, we observe two overlapping high-order multiplets, one for the 4 Cp α-protons (*para*-substituted Cp ring) and the 4 Cp α'-protons (*meta*-substituted Cp ring) that resonate at δ = 4.59 ppm, and a further high-order multiplet for 8 Cp β-protons at δ = 4.39 ppm. The observed spectrum reflects the averaged conformation in fast exchange at the NMR time scale.

Gradual lowering of the temperature forces the revolving motion of the ferrocene joints to match the NMR time scale and hence differentiate the protons from interior and exterior position, in which all α-protons become anisochronous δ ($\alpha_{int} \neq \alpha_{ext} \neq \alpha'_{int} \neq \alpha'_{ext}$). Likewise, β-protons diverge into two signals with different chemical shift δ ($\beta_{int} = \beta'_{int}$) ≠ δ ($\beta_{ext} = \beta'_{ext}$). This splitting can be explained by the magnetic inequivalence of the two Cp rings due to the different substitution at the unsymmetric phenyl ring and the spatial variance of protons facing the exterior or interior of the macrocycle. The coalescence temperature (T_c = 186.7 ± 0.5 °K) was identified by line shape analysis (LSA) (see Supporting Information Figure S77) of β-protons and used to determine the rate constant of interconversion to be: $k_{eTc} \approx$ 71.0 s^{-1} with an activation energy of $\Delta G^{\ddagger}_{eTc}$ = 38.5 ± 2.2 kJ mol^{-1}, $\Delta H^{\ddagger}_{g}$= 44.8 ± 2.0 kJ mol^{-1} and $\Delta S^{\ddagger}_{g}$ = 34.0 ± 1.6 J K^{-1} mol^{-1}. The positive entropy term suggests a transition state with reduced symmetry (see Supporting Information Figure S10).

It is noteworthy that similar dangling motions of ferrocene subunits heteroannularly integrated in macrocycles have already been reported, like e.g. the helical ferrocene porphyrinoids reported by Stępień et al.[29]

DFT calculations.

To get a better insight into the energies involved in the revolving motion of the Fc subunits analyzed by the VT NMR experiment discussed above, the rotational barrier was estimated by calculating the energy content of three extreme conformers (see Figure 4). Namely, the starting point of the coplanar *rhomboid* **2** with C_i symmetry, the "helical" macrocycle with pseudo C_2 symmetry as end point of a single Fc subunit 180° rotation, and the transition state with a rotation of the moving Fc subunit of about 90°, which was considered as proxy for the highest point in the energetic landscape between both conformers. The geometries of the coplanar and the helical conformer of *rhomboid* **2** were optimized. Calculations were carried out using the Gaussian09 suite of codes[30], on the B3LYP level of theory using a mixed basis set. C, H, S atoms were treated with 6-31G** whereas Fe was treated with the LANL2DZ basis set.[31,32] The transition state with one Fc subunits perpendicular to the second one, was located using the Synchronous Transit Guided Quasi-Newton (STQN) method.[33] As already expected from the VT NMR experiment, very comparable energy contents were obtained for the two conformers, with the relaxed "helical" ground state conformer being 3.6 kJ mol^{-1} above the "coplanar" ground state structure. With $\Delta E^{\ddagger}$ = 70.1 kJ mol^{-1}, the calculated activation energy of the Fc revolving motion is of comparable dimension as the Gibbs free energy value $\Delta G^{\ddagger}$ = 38.5 kJ mol^{-1} obtained by the VT NMR experiment. The lower value obtained experimentally might be explained by the solvation of the transition state in the NMR experiment, which is not considered in the DFT calculation.

In conclusion, the analysis of the variable temperature NMR spectra and their comparison with calculated values fully corroborated not only the rhomboidal arrangement of the *rhomboid* **2**, but also the second part of our starting hypothesis, namely that the bulkiness of the peripheral substituents steers the conformational equilibrium and thereby determines the product formed in the ring closing C-C coupling reaction (see Scheme 1).

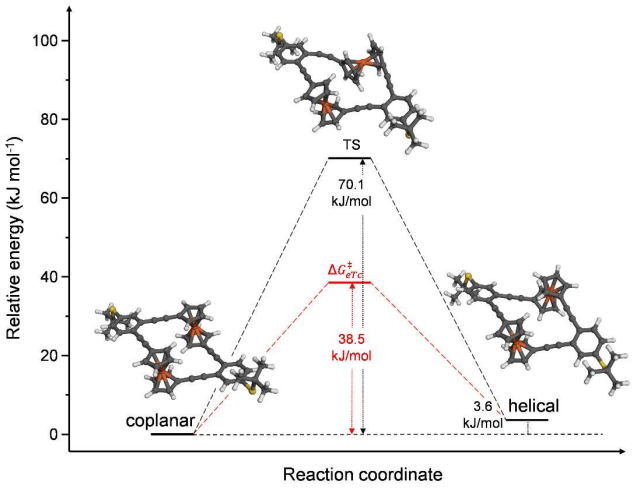

Figure 4. Relative energy diagram of the calculated conformers of the macrocycle **2** together with the Gibbs free energy of the transition state obtained by the VT NMR experiment in red.

Electrochemical analysis.

Both *bis*-ferrocene metallacycles, the *deltoid* **1** and the *rhomboid* **2**, consist of two ferrocene subunits which are each interlinked with both Cp units by *ortho*-diethynylbenzene connections. While the separation of both Fc subunits is comparable in both structures, the mobility of each Fc subunit within the framework of the metallacycle alters considerably, as already discussed in the section before. As the Fc joints are at the same time the redox-active subunits of both structures, their electrochemical investigation was of particular interest.

The redox properties of **1** and **2** were first studied using cyclic voltammetry (CV) and square wave voltammetry (SWV) in CH_2Cl_2 using *n*-Bu_4NPF_6 as the supporting electrolyte. The results are displayed in Figure 5 and summarized in Table 1. For compound **1** a single, reversible oxidation wave ($i_{pa}/i_{pc} \approx 1$, $i_p \propto v_s^{1/2}$ see Supporting Information Figure S4) at $E_{1/2}$ = 0.63 V vs. SCE is observed (Figure 5a) and formally attributed to the overlapping but sequential oxidation of both Fe^{II} centres to Fe^{III}. In the case of *bis*-ferrocene **2**, two irreversible oxidation waves were observed at E_{1Pa} = 0.63 V and E_{2Pa} = 1.68 V vs. SCE when scanning up to 1.8 V (Figure 5b).

Such reversibility challenges are well known from studies on multi-ferrocenyl compounds when *n*-Bu_4NPF_6 in CH_2Cl_2 is used.[34,35] When scanning up to 1.4 V vs. SCE only a single, reversible ($i_{pa}/i_{pc} \approx 1$, $i_p \propto v_s^{1/2}$, see Supporting Information Figure S5), two-electron oxidation wave was detected (Figure 5c). In literature, single-step multiple-electron transfers are common for multi-ferrocene complexes when a $[PF_6]^-$ salt is employed.[36–41] Diallo et. al deduced thereof that strong ion-pairing as facilitated by nucleophilic $[PF_6]^-$ ions, shield the electrostatic interaction between two redox centers and hence low electronic coupling between those redox centers leads to independent response.

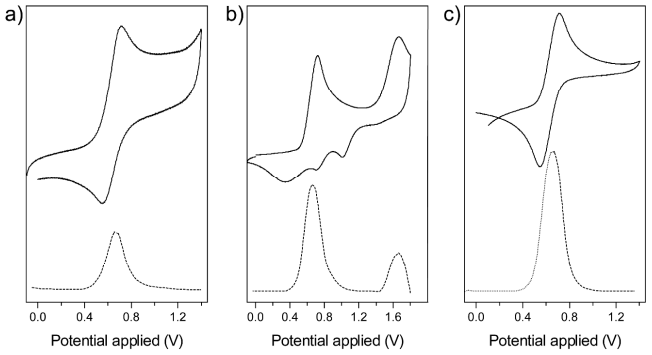

Figure 5. CV and SWV (dashed lines) curves of **1** a) and **2** c) with *n*-Bu_4NPF_6 as supporting electrolyte in DCM at 25 °C. The curve in b) further displays the irreversible behavior of **2** when a wide potential window is exploited.

Consequently, if a single redox wave is observed, low electronic through-bond communication between the redox centers can be assumed. This is in accordance with the single redox wave recorded for fully conjugated 1,2-*bis*-(ferrocenylethynyl)-benzene, when *n*-Bu_4NPF_6 in CH_2Cl_2 is used.[16]

Barrière and Geiger reported that using a perfluorinated electrolytes such as BARF = *tetrakis*[3,5-*bis*(trifluoromethyl)-phenyl]-borate weakens ion-pairing effects and favors the observation of electrostatic through-space communication.[42] Consequently, we recorded CV and SWV voltammograms of *bis*-ferrocene **1** and **2** with NaBARF as supporting electrolyte in CH_2Cl_2 (Figure 6). In the case of compound **2** a well-resolved two one-electron redox curve was recorded with half-wave potentials at $E_{1/2}$ = 0.13 V and $E_{1/2}$ = 0.41 V vs. SCE (Figure 6b). Each redox event exhibits reversible behavior ($i_{pa}/i_{pc} \approx 1$, $i_p \propto v_s^{1/2}$, see Supporting Information Figure S5 and S6, respectively) and voltammograms of *bis*-ferreocene **1** displays a broad wave, with a lowered half-wave potential at $E_{1/2}$ = 0.53 V vs. SCE (Figure 6a).

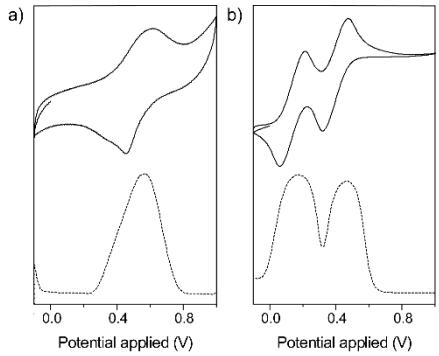

Figure 6. CV and SWV (dashed lines) curves of **1** a) and **2** b) with NaBARF as supporting electrolyte in CH_2Cl_2 vs. SCE at 25 °C

This seemingly complementary characteristic can be explained with the structure of the compounds. In the neutral form, the ferrocenes in **1** are relaxed and have no motivation to obtain opposing sides.

Table 1. Half-Wave Potentials ($E_{1/2}$) = (E_{pa} – E_{pc})/2, SWV Potentials in parenthesis for complex 2 and 3 in CH_2Cl_2 + *n*-Bu_4NPF_6 0.1 M or NaBARF 0.005 M.[a]

complex	$E_{1/2}$ *n*Bu_4NPF_6	$E_{1/2}$ NaBARF	$E_{1/2}$ NaBARF
1	0.63 (0.67)	0.54 (0.56)	-
2	0.63 (0.66)	0.13 (0.18)	0.41 (0.46)

[a]Glassy Carbon WE Ø = 2 mm, ν = 0.1 V s^{-1}, *E* vs. SCE in CH_2Cl_2 at 25 °C with the respective electrolyte.

When the redox centers are oxidized, the Coulomb repulsion between the two Fe^{III} atoms, forces them to turn out of plane. Obviously, the rigid structure of **1** doesn't facilitate free rotation along the Cp-sp single bonds. Twisting comes along with high conformational stress, which slows down the electron transfer rate and consequently broadens the redox wave. In Contrast, *bis*-ferrocene **2** showed to have highly flexible ferrocene joints that can freely twist, thereby reducing electrostatic repulsion which permits fast and sequential oxidation. These results allow to tentatively conclude that: First, the electronic through-bond communication between the two ferrocenes in **1** and **2** is insignificant, which consequently provide a framework capable of supporting charge localization, evident by ab-

sent wave splitting in a $[PF_6]^-$ electrolyte media. Second, the large half-wave potential split in compound **2** of $\Delta E_{1/2}$ = 280 mV and the broadened redox wave in *bis*-ferrocene **1** suggest considerable through-space communication when BARF is employed as electrolyte. These characteristics deliver the essentials for field-coupled applications in material science.[37,43,44]

Conclusion.

Two new *bis*-ferrocene macrocycles are presented, namely the rigid C_2 symmetric *deltoid* molecule **1** and the *rhomboidal* shaped *bis*-ferrocene **2**. Both are assembled by very similar Sonogashira-type coupling chemistry with tuned steric interactions in the ring closing step as decider whether the *deltoid* or the *rhomboid* structure is formed. While the identity of **1** is corroborated by its solid-state structure, only the *rhomboid* **2** is able to allow for revolving motions of the ferrocene-subunits which was observed by VT NMR studies. Electrochemical investigations of **1** and **2** display through space electrostatic interaction between both ferrocene-subunits for both macrocycles.

We are currently investigating the potential of such *rhomboid bis*-ferrocene macrocycles as electrochemically triggered single molecule mechanical transformers.

ASSOCIATED CONTENT

Supporting Information available free of charge via the Internet at http://pubs.acs.org.: General details, synthesis and spectroscopic data and copies of ^{1}H and ^{13}C NMR spectra of new compounds. Experimental details on electrochemical measurements. Crystal data and structure refinement of compound **1**. Further details on theoretical calculations and Cartesian coordinates of computed structures of **2**. Copies of VT NMR, 2D NMR and HRMS spectra of new compounds are displayed. CCDC 1515120 and crystallographic data in CIF format.

AUTHOR INFORMATION

Corresponding Author

*marcel.mayor@unibas.ch

Notes

The authors declare no competing financial interest.

ACKNOWLEDGMENTS

The authors thank the Swiss National Science Foundation (SNF) (grant number 200020-159730) for continuous and generous financial support.

REFERENCES

(1) Muraoka, T.; Kinbara, K.; Kobayashi, Y.; Aida, T. *J. Am. Chem. Soc.* **2003**, *125* (19), 5612–5613.
(2) Lima, C. F. R. A. C.; Fernandes, A. M.; Melo, A.; Gonçalves, L. M.; Silva, A. M. S.; Santos, L. M. N. B. F. *Phys. Chem. Chem. Phys.* **2015**, *17* (37), 23917–23923.
(3) Ikeda, T.; Shinkai, S.; Sada, K.; Takeuchi, M. *Tetrahedron Lett.* **2009**, *50* (17), 2006–2009.
(4) Fukino, T.; Fujita, N.; Aida, T. *Org. Lett.* **2010**, *12* (13), 3074–3077.
(5) Katz, T. J.; Pesti, J. *J. Am. Chem. Soc.* **1982**, *104* (1), 346–347.
(6) Lu, Q.; Yao, C.; Wang, X.; Wang, F. *J. Phys. Chem. C* **2012**, *116* (33), 17853–17861.
(7) Lim, J. Y. C.; Cunningham, M. J.; Davis, J. J.; Beer, P. D. *Chem. Commun.* **2015**, *51* (78), 14640–14643.
(8) Xiao, X.; Brune, D.; He, J.; Lindsay, S.; Gorman, C. B.; Tao, N. *Chem. Phys.* **2006**, *326* (1), 138–143.
(9) Hoffmann, V.; Jenny, N.; Häussinger, D.; Neuburger, M.; Mayor, M. *Eur. J. Org. Chem.* **2016**, *2016* (12), 2187–2199.
(10) Weibel, N.; Mishchenko, A.; Wandlowski, T.; Neuburger, M.; Leroux, Y.; Mayor, M. *Eur. J. Org. Chem.* **2009**, *2009* (35), 6140–6150.
(11) Shu, L.; Müri, M.; Krupke, R.; Mayor, M. *Org. Biomol. Chem.* **2009**, *7* (6), 1081.
(12) Błaszczyk, A.; Chadim, M.; von Hänisch, C.; Mayor, M. *Eur. J. Org. Chem.* **2006**, *2006* (17), 3809–3825.
(13) Shu, L.; Mayor, M. *Chem. Commun.* **2006**, No. 39, 4134.
(14) Mayor, M.; Didschies, C. *Angew. Chem. Int. Ed.* **2003**, *42* (27), 3176–3179.
(15) Mayor, M.; Lehn, J.-M. *J. Am. Chem. Soc.* **1999**, *121* (48), 11231–11232.
(16) Diallo, A. K.; Absalon, C.; Ruiz, J.; Astruc, D. *J. Am. Chem. Soc.* **2011**, *133* (3), 629–641.
(17) Ingham, S. L.; Khan, M. S.; Lewis, J.; Long, N. J.; Raithby, P. R. *J. Organomet. Chem.* **1994**, *470* (1–2), 153–159.
(18) Inkpen, M. S.; White, A. J. P.; Albrecht, T.; Long, N. J. *Dalton Trans.* **2014**, *43* (41), 15287–15290.
(19) Jenny, N. M.; Mayor, M.; Eaton, T. R. *Eur. J. Org. Chem.* **2011**, *2011* (26), 4965–4983.
(20) Baumgardt, I.; Butenschön, H. *Eur. J. Org. Chem.* **2010**, *2010* (6), 1076–1087.
(21) Inkpen, M. S.; White, A. J. P.; Albrecht, T.; Long, N. J. *Chem. Commun.* **2013**, *49* (50), 5663–5665.
(22) Krauße, N.; Kielmann, M.; Ma, J.; Butenschön, H. *Eur. J. Org. Chem.* **2015**, *2015* (12), 2622–2631.
(23) Kukula, H.; Veit, S.; Godt, A. *Eur. J. Org. Chem.* **1999**, *1999* (1), 277–286.
(24) Hundertmark, T.; Littke, A. F.; Buchwald, S. L.; Fu, G. C. *Org. Lett.* **2000**, *2* (12), 1729–1731.
(25) Netherton, M. R.; Fu, G. C. *Org. Lett.* **2001**, *3* (26), 4295–4298.
(26) Abel, E. W.; Long, N. J.; Orrell, K. G.; Osborne, A. G.; Šik, V. *J. Organomet. Chem.* **1991**, *403* (1–2), 195–208.
(27) Wu, G.; Liu, Q.; Shen, Y.; Wu, W.; Wu, L. *Tetrahedron Lett.* **2005**, *46* (35), 5831–5834.
(28) Doyle, M. P.; Siegfried, B.; Dellaria, J. F. *J. Org. Chem.* **1977**, *42* (14), 2426–2431.
(29) Stępień, M.; Simkowa, I.; Latos-Grażyński, L. *Eur. J. Org. Chem.* **2008**, *2008* (15), 2601–2611.
(30) M. J. Frisch, G. W. Trucks, H. B. Schlegel, G. E. Scuseria, M. A. Robb, J. R. Cheeseman, G. Scalmani, V. Barone, B. Mennucci, G. A. Petersson, H. Nakatsuji, M. Caricato, X. Li, H. P. Hratchian, A. F. Izmaylov, J. Bloino, G. Zheng, J. L. Sonnenberg, M. Hada, M. Ehara, K. Toyota, R. Fukuda, J. Hasegawa, M. Ishida, T. Nakajima, Y. Honda, O. Kitao, H. Nakai, T. Vreven, J. A. Montgomery, Jr., J. E. Peralta, F. Ogliaro, M. Bearpark, J. J. Heyd, E. Brothers, K. N. Kudin, V. N. Staroverov, R. Kobayashi, J. Normand, K. Raghavachari, A. Rendell, J. C. Burant, S. S. Iyengar, J. Tomasi, M. Cossi, N. Rega, J. M. Millam, M. Klene, J. E. Knox, J. B. Cross, V. Bakken, C. Adamo, J. Jaramillo, R. Gomperts, R. E. Stratmann, O. Yazyev, A. J. Austin, R. Cammi, C. Pomelli, J. W. Ochterski, R. L. Martin, K. Morokuma, V. G.

Zakrzewski, G. A. Voth, P. Salvador, J. J. Dannenberg, S. Dapprich, A. D. Daniels, Ö. Farkas, J. B. Foresman, J. V. Ortiz, J. Cioslowski, and D. J. Fox. *Gaussian 09*; Gaussian Inc.: Wellington, CT, 2009.
(31) Ditchfield, R.; Hehre, W. J.; Pople, J. A. *J. Chem. Phys.* **1971**, *54* (2), 724–728.
(32) Hay, P. J.; Wadt, W. R. *J. Chem. Phys.* **1985**, *82* (1), 299–310.
(33) Peng, C.; Bernhard Schlegel, H. *Isr. J. Chem.* **1993**, *33* (4), 449–454.
(34) Inkpen, M. S.; Scheerer, S.; Linseis, M.; White, A. J. P.; Winter, R. F.; Albrecht, T.; Long, N. J. *Nat. Chem.* **2016**, *advance online publication*.
(35) Geiger, W. E.; Barrière, F. *Acc. Chem. Res.* **2010**, *43* (7), 1030–1039.
(36) Ou-Yang, J.-K.; Chen, L.-J.; Xu, L.; Wang, C.-H.; Yang, H.-B. *Chin. Chem. Lett.* **2013**, *24* (6), 471–474.
(37) Arima, V.; Iurlo, M.; Zoli, L.; Kumar, S.; Piacenza, M.; Sala, F. D.; Matino, F.; Maruccio, G.; Rinaldi, R.; Paolucci, F.; Marcaccio, M.; Cozzi, P. G.; Bramanti, A. P. *Nanoscale* **2012**, *4* (3), 813–823.
(38) Das, N.; Arif, A. M.; Stang, P. J.; Sieger, M.; Sarkar, B.; Kaim, W.; Fiedler, J. *Inorg. Chem.* **2005**, *44* (16), 5798–5804.
(39) Fillaut, J.-L.; Astruc, D.; Linares, J. *Angew. Chem. Int. Ed. Engl.* **1995**, *33* (23–24), 2460–2462.
(40) Chebny, V. J.; Dhar, D.; Lindeman, S. V.; Rathore, R. *Org. Lett.* **2006**, *8* (22), 5041–5044.
(41) Diallo, A. K.; Daran, J.-C.; Varret, F.; Ruiz, J.; Astruc, D. *Angew. Chem. Int. Ed.* **2009**, *48* (17), 3141–3145.
(42) Barrière, F.; Geiger, W. E. *J. Am. Chem. Soc.* **2006**, *128* (12), 3980–3989.
(43) Lent, C. S.; Tougaw, P. D.; Porod, W.; Bernstein, G. H. *Nanotechnology* **1993**, *4* (1), 49.
(44) Schneider, B.; Demeshko, S.; Neudeck, S.; Dechert, S.; Meyer, F. *Inorg. Chem.* **2013**, *52* (22), 13230–13237.

Table of Contents artwork

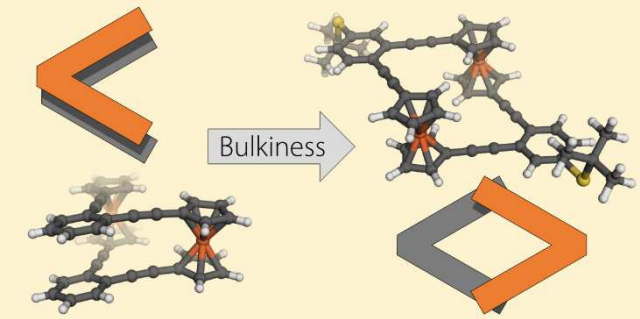

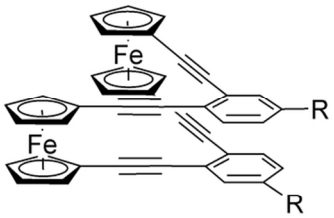

1 : R = H
"deltoid"

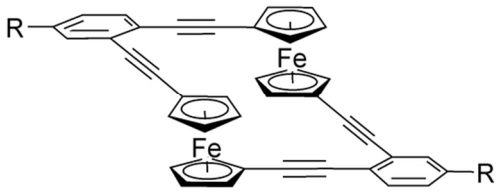

2 : R = $SC(CH_3)_3$
"rhomboid"

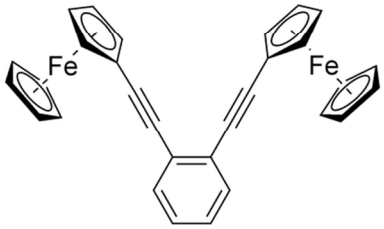

3
1,2-bis(ferrocenylethynyl)-benzene

92x62mm (300 x 300 DPI)

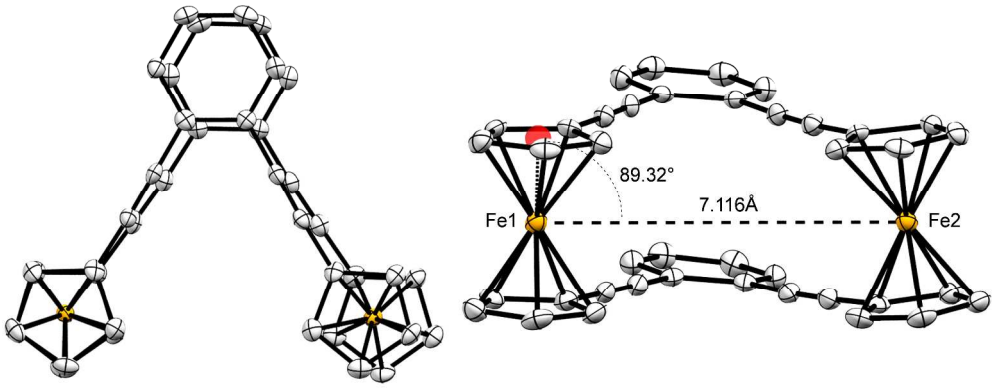

1387x542mm (144 x 144 DPI)

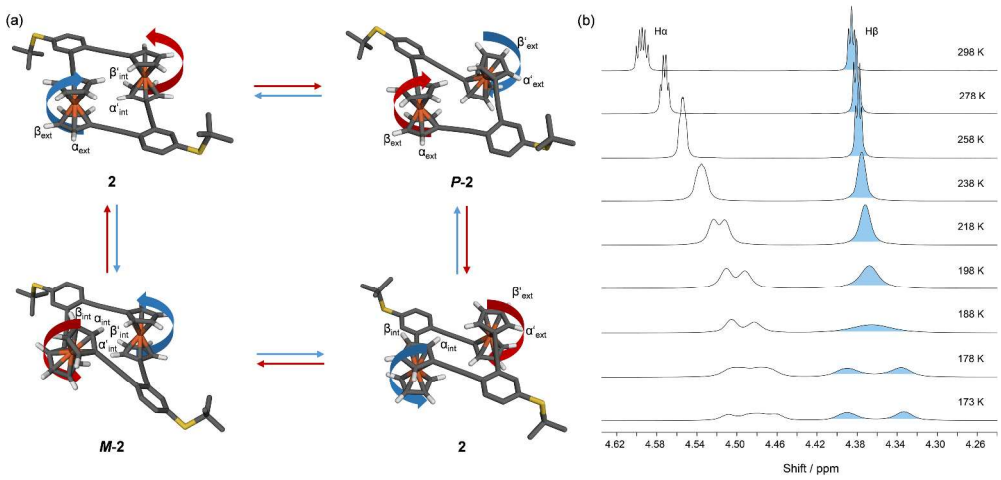

1205x567mm (144 x 144 DPI)

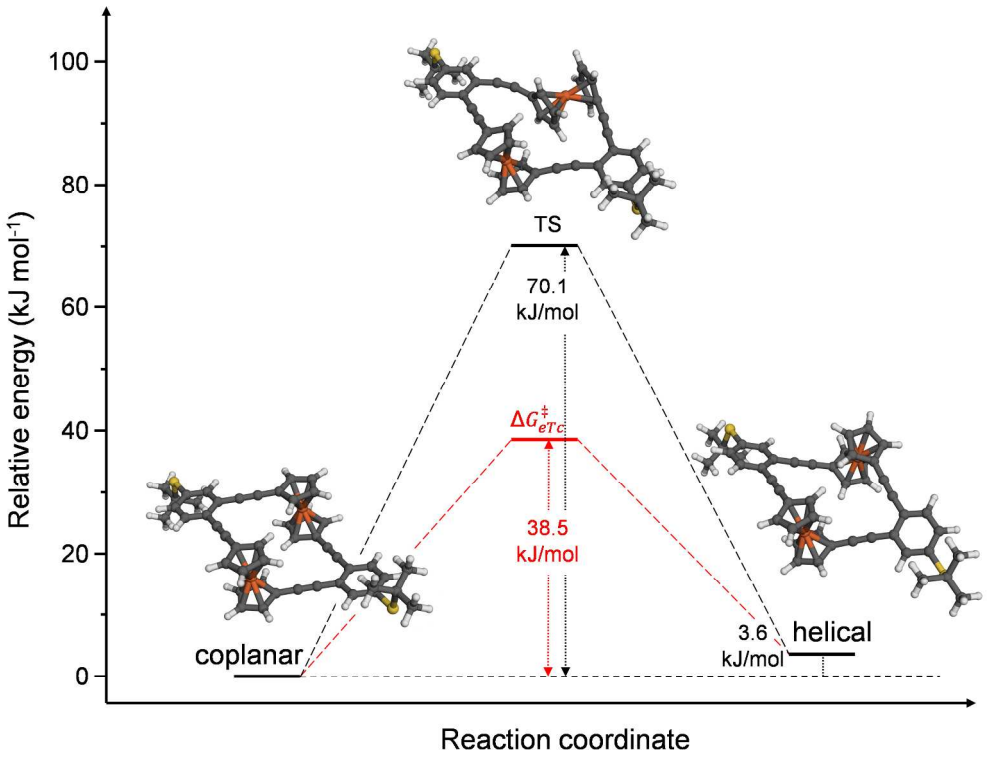

473x367mm (144 x 144 DPI)

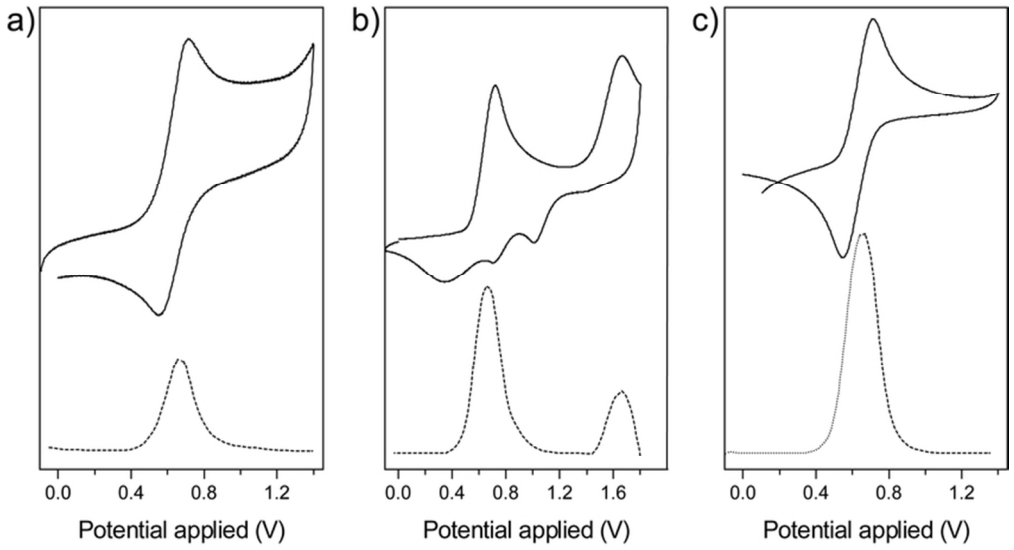

71x38mm (300 x 300 DPI)

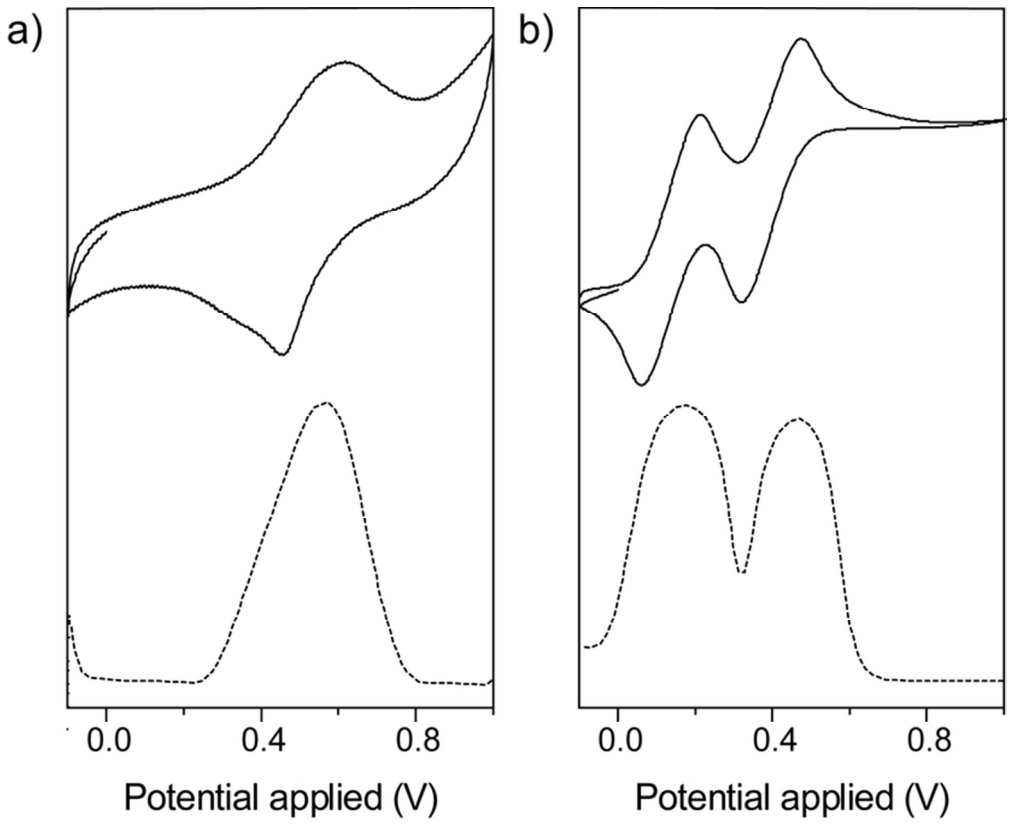

70x57mm (300 x 300 DPI)

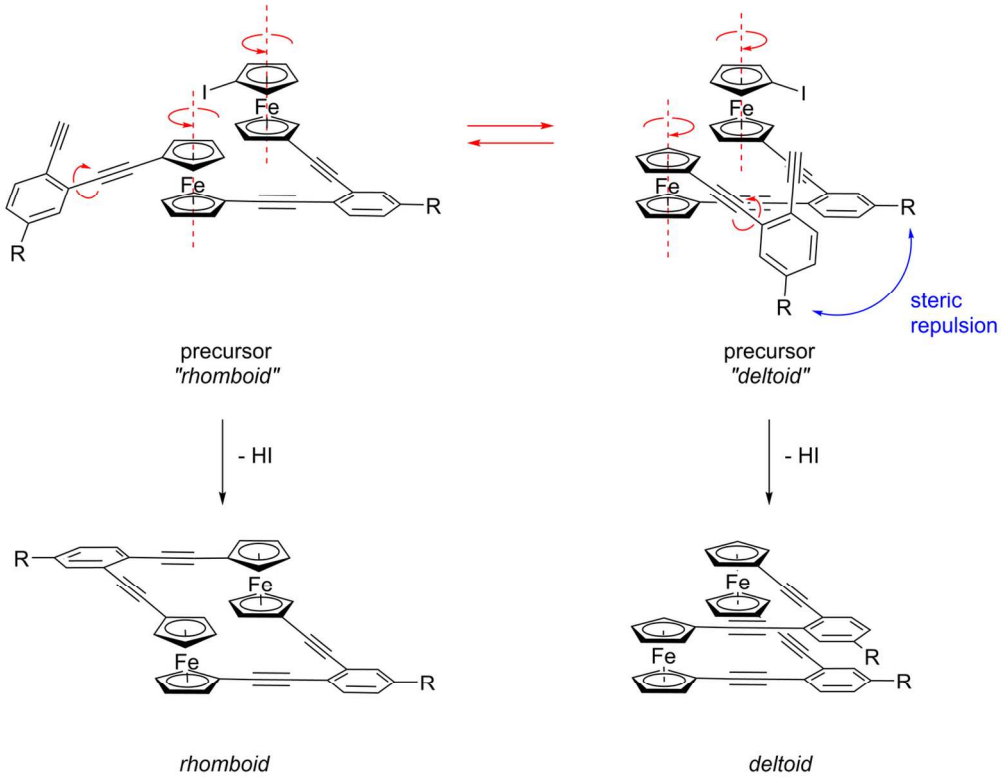

127x99mm (300 x 300 DPI)

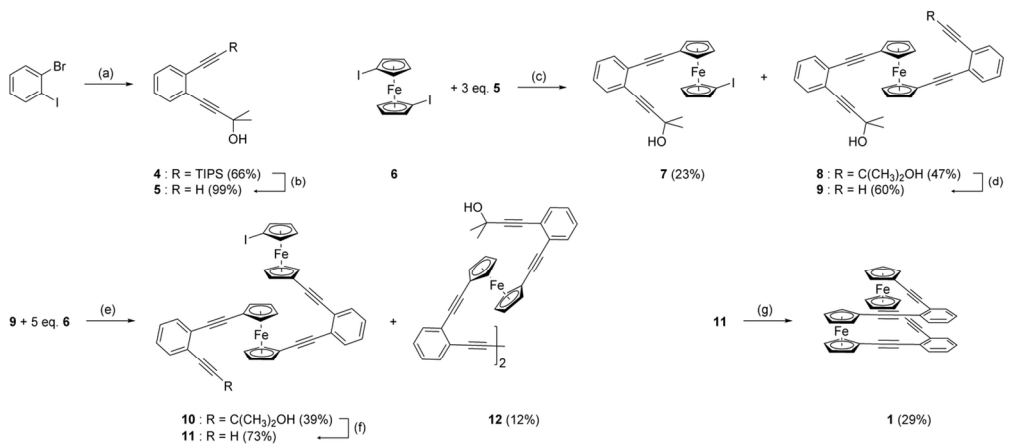

121x53mm (300 x 300 DPI)

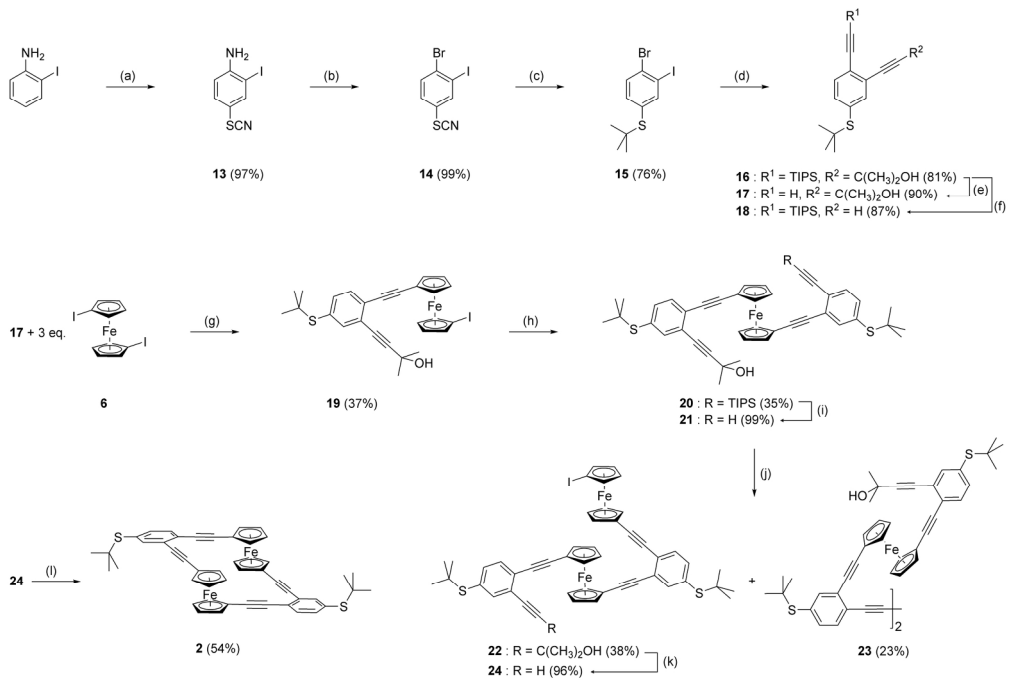

188x127mm (300 x 300 DPI)

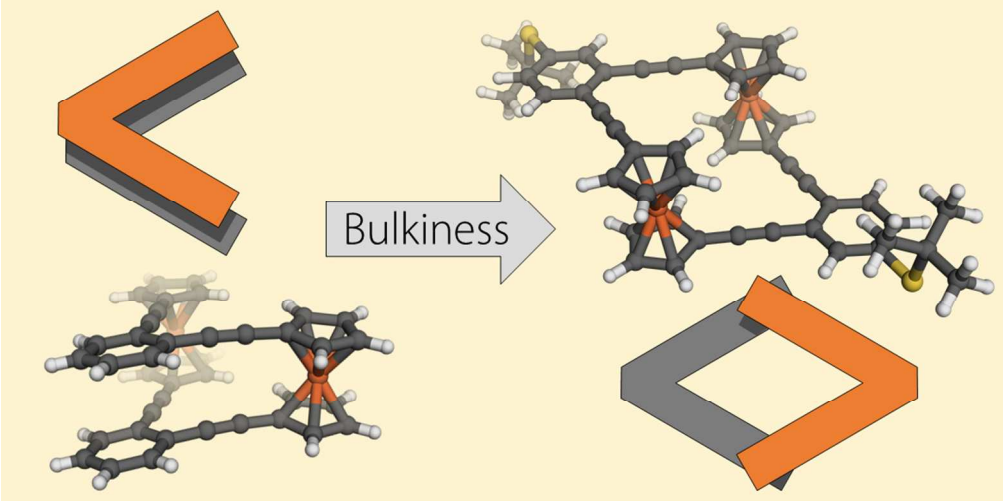

307x153mm (96 x 96 DPI)